LETTERS
PUBLISHED ONLINE: 1 DECEMBER 2013 | DOI: 10.1038/NGEO2021
nature geoscience

Ocean-driven heating of Europa's icy shell at low latitudes

K. M. Soderlund[1]*, B. E. Schmidt[1,2], J. Wicht[3] and D. D. Blankenship[1]

The ice shell of Jupiter's moon Europa is marked by regions of disrupted ice known as chaos terrains that cover up to 40% of the satellite's surface, most commonly occurring within 40° of the equator[1]. Concurrence with salt deposits[2] implies a coupling between the geologically active ice shell and the underlying liquid water ocean at lower latitudes. Europa's ocean dynamics have been assumed to adopt a two-dimensional pattern[3–8], which channels the moon's internal heat to higher latitudes. Here we present a numerical model of thermal convection in a thin, rotating spherical shell where small-scale convection instead adopts a three-dimensional structure and is more vigorous at lower latitudes. Global-scale currents are organized into three zonal jets and two equatorial Hadley-like circulation cells. We find that these convective motions transmit Europa's internal heat towards the surface most effectively in equatorial regions, where they can directly influence the thermo-compositional state and structure of the ice shell. We suggest that such heterogeneous heating promotes the formation of chaos features through increased melting of the ice shell and subsequent deposition of marine ice at low latitudes. We conclude that Europa's ocean dynamics can modulate the exchange of heat and materials between the surface and interior and explain the observed distribution of chaos terrains.

Although magnetometer measurements by the Galileo spacecraft have shown Europa to have a global ocean[9], no direct oceanographic measurements are available. Surface geology, however, may be an indicator of Europa's internal dynamics (see Supplementary Section 1 and Fig. 1). The origin of chaos features is strongly debated[10], but heat transferred from the underlying ocean and/or produced by tidal dissipation is expected to be critical—either to melt through a thin ice shell[3,4,11] or to initiate solid-state convection in a thick ice shell[12–14]. Radiogenic and tidal heating in the mantle, as well as secular cooling, amount to a sizable fraction of the net heat flux emanated from the satellite that must be transferred through the ocean[15]. This can be achieved only by vigorous ocean convection whose particular dynamics determine the lateral heat flux variations along the base of the ice shell. Eccentricity-induced tidal heating within the ice shell peaks at high latitudes[16] and is thus unable to explain the distribution of chaos terrain without appealing to other factors such as obliquity tides, non-uniform ice shell properties or polar wander. We, therefore, argue that ocean dynamics may play a decisive role for Europan surface geology.

The Coriolis force in rapidly rotating systems typically organizes convective flows into quasi-two-dimensional (2D) structures called Taylor columns that are aligned with the rotation axis (Fig. 1a). If this style of convection rules the dynamics in Europa's ocean, associated Reynolds stresses would drive an eastward equatorial jet flanked by multiple zonal jets of alternating direction[17]. Furthermore, secondary axial flows in the Taylor columns and efficient thermal plumes near the poles would maximize global heat transport at high latitudes[18], which is inconsistent with the observed provenance of chaos terrain. However, when convective driving is strong enough and the flow sufficiently vigorous, the Coriolis force loses its ordering influence and convection becomes more turbulent and quasi-3D (Fig. 1b,c). Our simulations demonstrate that the zonal flows and heat flow also differ markedly from rotationally constrained dynamics.

Classically, the transition between these two regimes is assumed to occur at $Ro_c \approx 1$, where the convective Rossby number Ro_c measures the global ratio of convective driving to Coriolis forces. For many planetary applications, Ro_c is much smaller than unity such that quasi-2D Taylor column-like motions are expected to prevail. Estimates for the convective Rossby number in Europa's ocean reach from about 0.01 to 1 (see Supplementary Section 2). Previous authors have adopted small values more typical for convection in other planetary bodies and thereby assumed columnar dynamics[3–8]. However, the upper estimate of $Ro_c \approx 1$ suggests that quasi-3D turbulence may already play a significant role for Europa's ocean. Recent studies of rotating Rayleigh–Bénard convection[19,20] also suggest that the transition may happen even for convective Rossby numbers significantly smaller than one (Supplementary Fig. 2), which further supports the hypothesis that rotation can play only a minor role in organizing convection. This alternative convective mode, which has not been investigated previously in the context of Europa's ocean, implies not only a different dynamic regime but also a different zonal flow pattern and thermal signature than commonly assumed[3–8] (Fig. 1).

We use a numerical model of thermal convection in a rotating spherical shell to test the implications of a dynamical regime beyond the transition to 3D turbulence. The control parameters of the model are consistent with our understanding of Europa's interior (Methods). Snapshots of axial vorticity isosurfaces (Fig. 1c) and radial flows at mid-depth (Fig. 2a) illustrate the rather small-scale and highly dynamic convective structure without any tendency to form columns. However, radial flow amplitudes are clearly higher at lower latitudes. Time averages also reveal that the radial flow is predominantly directed outward near the equator and inward at higher latitudes (Fig. 2b), creating meridional circulations with poleward flow along the ice–ocean interface and equatorward return flow near the sea floor. As shown in Figs 1c and 2c, the zonal flow is dominated by three jets produced by homogenization of total angular momentum due to efficient convective mixing[21,22]. Mean radial current speeds are $\sim 3\,\mathrm{cm\,s^{-1}}$ and zonal speeds are typically $\sim 250\,\mathrm{cm\,s^{-1}}$. For comparison, ocean currents in the Gulf Stream can exceed $1\,\mathrm{m\,s^{-1}}$ (although driven by winds rather than

[1]Institute for Geophysics, John A. & Katherine G. Jackson School of Geosciences, The University of Texas at Austin, J. J. Pickle Research Campus, Building 196 (ROC), 10100 Burnet Road (R2200), Austin, Texas 78758-4445, USA, [2]School of Earth and Atmospheric Sciences, Georgia Institute of Technology, 311 Ferst Drive, Atlanta, Georgia 30332-0340, USA, [3]Max Planck Institute for Solar System Research, Katlenburg-Lindau 37191, Germany.
*e-mail: krista@ig.utexas.edu

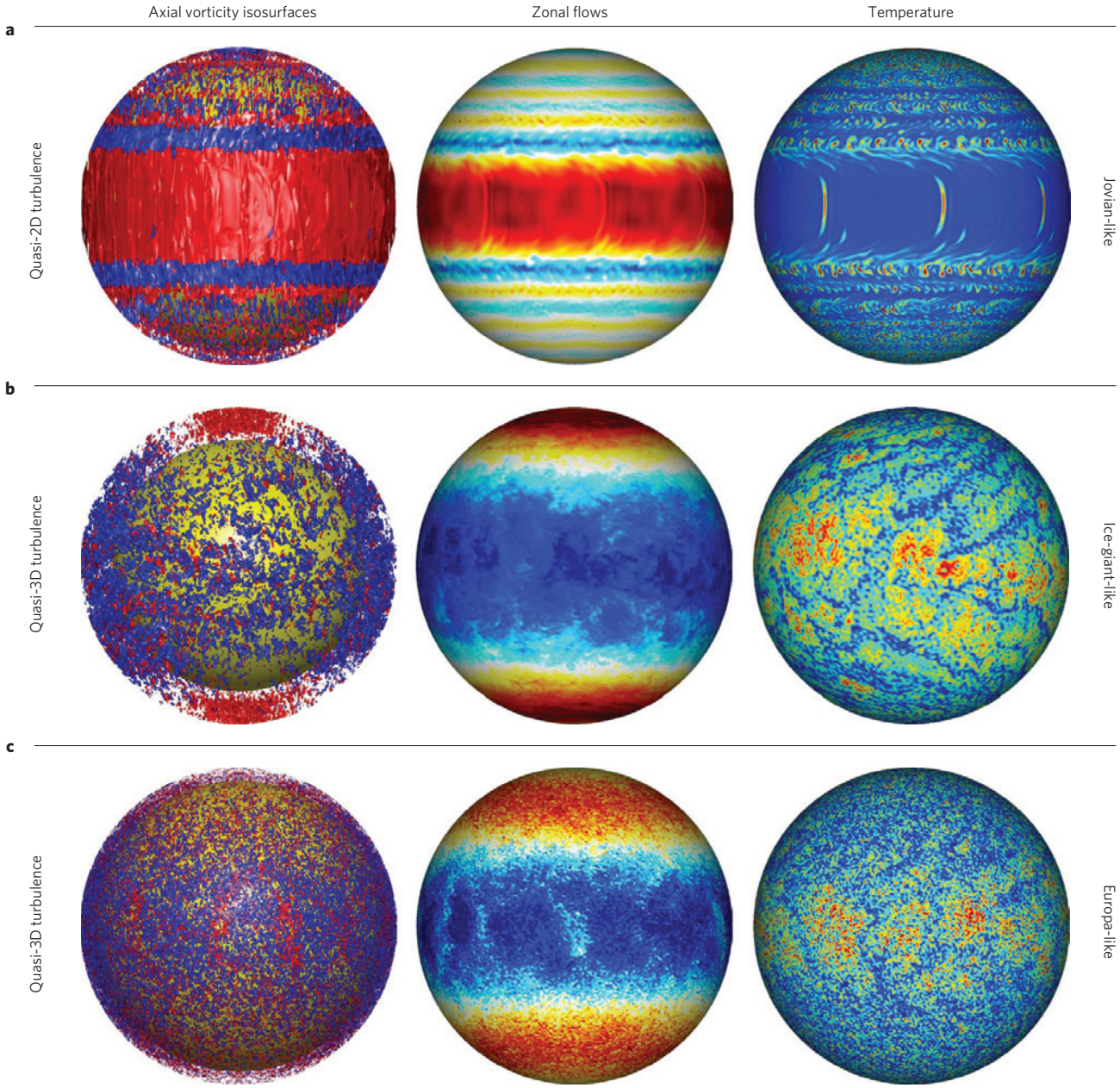

Figure 1 | Convective flow structures, zonal flows and temperature fields in planetary convection models. Left: instantaneous isosurfaces of axial vorticity, $\omega_z = (\nabla x u) \cdot \hat{Z}$, in the bulk fluid. Red (blue) indicates cyclonic (anticyclonic) vorticity; the yellow sphere represents the mantle. Middle: instantaneous zonal flows along the outer boundary, r_o, where red (blue) indicates prograde (retrograde) flow. Right: instantaneous superadiabatic temperature fields at $r = 0.99r_o$, where red (blue) indicates warm (cool) fluid. **a**, Jovian-like simulation from refs 17,18 (data provided by M. H. Heimpel). **b**, Ice-giant-like simulation from ref. 22. **c**, Our Europa-like ocean simulation. Control parameters are given in Supplementary Table 1.

convection). Our results imply that these jets are probably present in Europa's ocean, with a westward jet at low latitudes and eastward jets at high latitudes, and that two equatorial Hadley-like cells control the meridional circulations.

Fluid motions beneath Europa's ice shell are intrinsically coupled to both the global and regional thermal behaviour. Figure 3a shows a snapshot of the simulated superadiabatic temperature field in the equatorial plane. Hotter thermal plumes that originate along the inner ocean boundary lose their identity as they rise through the ocean. On time average, the equatorial region convects more vigorously than the polar regions and therefore has a nearly homogeneous temperature (Fig. 3b). Consequently, more heat is delivered to the ice shell at low latitudes (Fig. 1c). Figure 4a demonstrates that this latitudinal dependence can even be discerned in temporal snapshots with higher than average heat flux regions (red patches) being concentrated at latitudes below $\pm 20°$. Supplementary Video 1 shows that these patches fluctuate rapidly in time yet retain this low-latitude concentration. When averaged in longitude and time (Fig. 4b), the heat flux varies by about 40% with a clear maximum at the equator and nearly uniform flux elsewhere. This delivery of more thermal flux to the ice shell near the equator promotes the likelihood of enhanced ocean-driven geologic activity in the ice shell for this region.

Our simulations imply that latitudinal heterogeneity in heat flux should intensify regional ice shell melting near the equator. If the ice shell is thin, low-latitude thinning of the ice shell would increase the likelihood for melt-through events proposed as one possible origin of chaos terrain[3,4,11]. However, any latitudinal thickness disparity

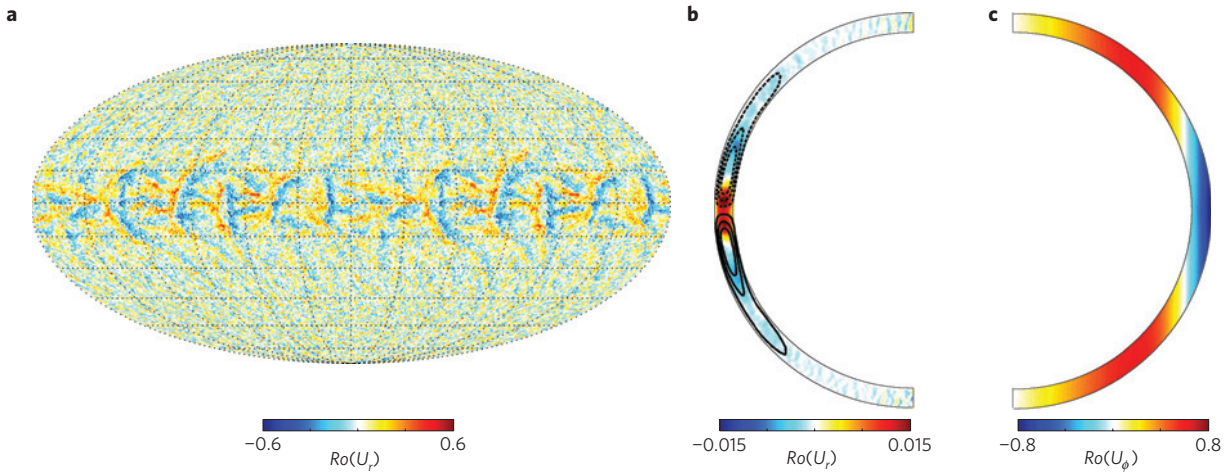

Figure 2 | Radial velocity, meridional circulations and zonal flows in our Europa-like ocean model. a, Instantaneous radial velocity field at $r = 0.95r_o$ (mid-ocean depth). Blue (red) indicates inward (outward) motions. **b**, Time-averaged, axisymmetric radial velocity field with superimposed contours of the stream function where solid (dashed) contours indicate anticlockwise (clockwise) meridional circulations. **c**, Time-averaged, axisymmetric zonal flows where blue (red) indicates westward (eastward) motions. All speeds are given in dimensionless Rossby number units, $Ro = U/(2\Omega D)$, and are therefore measured relative to the speed of rotation.

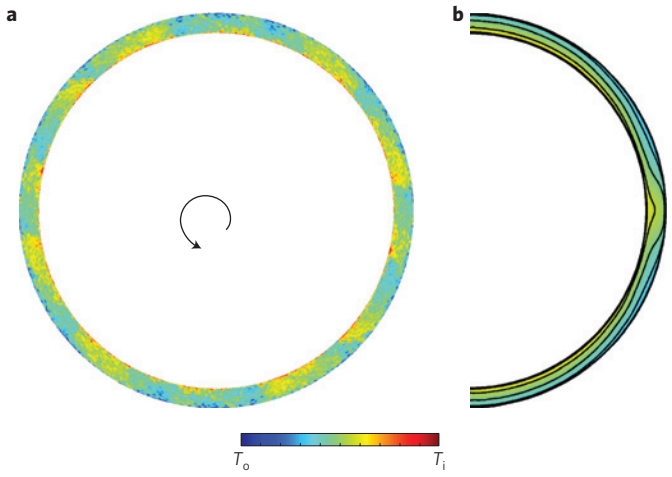

Figure 3 | Simulated ocean temperature distributions. a, Instantaneous temperature field in the equatorial plane as viewed from above. **b**, Time-averaged, axisymmetric temperature in the meridional (r,θ) plane with isotherms in black. Turbulence destroys coherent thermal plumes in the ocean, and the mean superadiabatic ocean temperature tends to be well mixed within the equatorial region. In both panels, temperature ranges from T_o on the outer ocean boundary to $T_i = T_o + \Delta T$ on the inner ocean boundary, where $T_o < T_i$. As the model is defined by the superadiabatic temperature contrast, ΔT, rather than absolute temperatures, T_o can be arbitrarily prescribed.

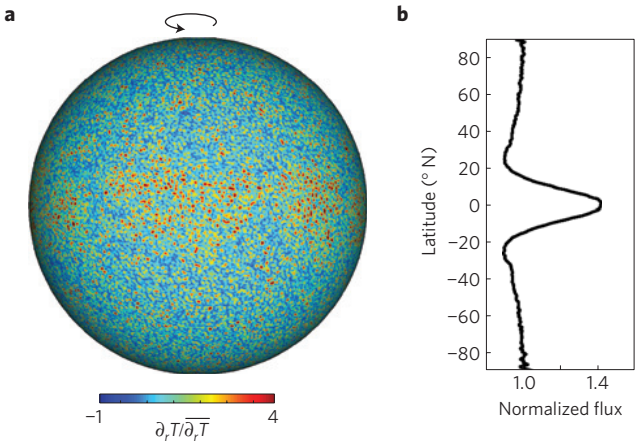

Figure 4 | Pattern of radial heat transfer. a, Instantaneous radial heat flux on the outer ocean boundary, normalized by the mean value. **b**, Time-averaged, axisymmetric radial heat flux at $r = r_o$ as a function of latitude, normalized by the mean value. Heat flux is achieved instantaneously through small-scale, short-lived patches driven by turbulence that are more prevalent near the equator. When averaged in time, this pattern results in high equatorial heat flux and low heat flux elsewhere along the outer ocean boundary, promoting equatorial melting of the ice shell.

will be limited by a thermohaline process known as an ice pump[23]. Pressure-induced melting under the thicker portions of the ice shell at higher latitudes will produce a layer of colder, freshened sea water that migrates to low-latitude regions of thinner ice where it freezes with a significant rejection (99.9%) of constituent impurities[24]. This accreted 'marine' ice then counteracts the heating-induced thickness disparity. Ice pumps are common in Antarctica and have produced more than a 50% contribution of marine ice to the total thickness of certain ice shelves[25]. Importantly, any substantial thickness of relatively pure, low-latitude marine ice on Europa may contribute to compositional diapirism, a potential trigger for the formation of chaos terrain in a thick ice shell[13,14]. In addition, the latitudinal redistribution of ice shell mass may have crucial implications for ice shell reorientation through polar wander. Although our results do not preclude the polar wander scenario, accreted marine ice is a phenomenon that can inhibit the ability of the ice shell to reorient because ice pumps modify the total ice thickness and dynamics of ice shelves on timescales that are much faster than ice flow[23,26].

In the absence of oceanographic measurements, new approaches are needed to better understand Europa's ocean. Our global ocean modelling shows that a pattern of oceanic heat transfer may exist for Europa that will strongly influence the evolution of the ice shell as well as any material exchange between the ocean and the ice shell. Furthermore, terrestrial analogues suggest that the ice shell composition may vary latitudinally through the accretion of marine ice, consistent with the detection of ocean-derived material on Europa's surface at low latitudes[2]. The upcoming JUICE (JUpiter

ICy moons Explorer) mission will also fly over Europa's chaos terrain and provide detailed measurements of the sub-surface ice structure and induced magnetic fields[27] to further constrain Europan ocean dynamics and the effects of ice–ocean coupling.

Methods

We simulate the dynamics of Europa's ocean using the pseudo-spectral code MagIC (ref. 28), which solves for thermal convection of a Boussinesq fluid in a rotating spherical shell. Four dimensionless parameters define the problem: the ratio of inner to outer ocean radii $\chi = r_i/r_o$ (system geometry), the Prandtl number $Pr = \nu/\kappa$ (ratio of viscous to thermal diffusivities), the Ekman number $E = \nu/(2\Omega D^2)$ (ratio of viscous to Coriolis forces), and the Rayleigh number $Ra = \alpha g \Delta T D^3/(\nu\kappa)$ (ratio of buoyancy to diffusive effects). We adopt terrestrial oceanographic values to characterize the physical properties of Europa's ocean (see Supplementary Table 2). An outer ocean radius $r_o \approx 1{,}550$ km and inner ocean radius $r_i \approx 1{,}450$ km provide $\chi \approx 0.94$. The difference $r_o - r_i \approx 100$ km is used as length scale D. Rotation rate $\Omega \approx 2.1 \times 10^{-5}$ s^{-1} and kinematic viscosity $\nu \approx 1.5 \times 10^{-6}$ m^2 s^{-1} suggest an Ekman number of $E \approx 4 \times 10^{-12}$. Thermal diffusivity $\kappa \approx 1.3 \times 10^{-7}$ m^2 s^{-1} provides $Pr \approx 12$. Gravitational acceleration $g \approx 1.3$ m s^{-2}, thermal expansivity $\alpha \approx 3 \times 10^{-4}$ K^{-1}, and superadiabatic temperature contrast $\Delta T = O$ (0.1–100) mK are required to calculate the Rayleigh number (see Supplementary Section 3). The resulting estimates range from $Ra = \mathcal{O}(10^{20})$ to $Ra = \mathcal{O}(10^{23})$.

Numerical limitations force us to chose a much too large Ekman number of $E = 1.5 \times 10^{-4}$. As length scales and timescales rapidly decrease with Ekman number, all similar numerical models suffer from this problem[28]. Nevertheless, such models have proved to be valuable tools for studying the processes that may be occurring in planetary interiors because the large-scale dynamics do not seem to be strongly affected by unresolved turbulence. The radius ratio is realistic with $\chi = 0.9$. We chose $Pr = 1$, a value expected when diffusivities reflect turbulent rather than molecular values, and adjust the Rayleigh number to $Ra = 3.4 \times 10^7$ to select transition parameters that are approximately in the ranges estimated for Europa as shown in Supplementary Table 1. These control parameters are also expressed as dimensional physical properties in Supplementary Table 2. All quantities are realistic with the notable exceptions of viscous and thermal diffusivities and, consequently, the superadiabatic temperature contrast, which are orders of magnitude too large and the root of the unrealistic E and Ra values (see Supplementary Section 3 for more discussion).

Our Boussinesq model does not take fluid property variations with depth into account. However, laboratory experiments of water with and without salt impurities at Europa-relevant pressures and temperatures[29] imply that the mean physical properties of Europa's ocean when averaged over the expected P–T range are not expected to differ by more than about 30% from the terrestrial ocean values employed here. Our estimates of the governing control parameters, Ra in particular, remain on the same order when the experimental values are assumed. Thus, we do not expect the dynamics to be strongly modified by variations in pressure, temperature or salinity. However, two caveats should be pointed out: our model does not accommodate a layer of stably stratified fluid near the ice–ocean interface that may develop if the coefficient of thermal expansion is negative or if large amounts of buoyant melt water are produced[4] and we do not include the onset of double-diffusive convection[6].

Fluid motions and heat sources derived from compositional buoyancy and orbital dynamics (for example, tides and libration) are neglected. The isothermal top boundary condition reflects the fact that ice is at the freezing point here while allowing for horizontal heat flux variations. Isothermal bottom boundary conditions are chosen for simplicity. Both boundaries are impenetrable, and stress-free flow conditions are chosen to exclude the effects of Ekman boundary layers, which are too thick at the large Ekman numbers assumed in the simulations[30]. We use 73 radial levels, 213 spherical harmonic modes, and assume no azimuthal symmetries. Hyperdiffusion is not employed.

Received 14 August 2013; accepted 30 October 2013; published online 1 December 2013

References

1. Figueredo, P. H. & Greeley, R. Resurfacing history of Europa from pole-to-pole geological mapping. *Icarus* **167,** 287–312 (2004).
2. Brown, M. E. & Hand, K. P. Salts and radiation products on the surface of Europa. *Astron. J.* **145,** 110–110 (2013).
3. Thomson, R. E. & Delaney, J. R. Evidence for a weakly stratified Europan ocean sustained by seafloor heat flux. *J. Geophys. Res.* **106,** 12355–12365 (2001).
4. Melosh, H. J., Ekholm, A. G., Showman, A. P. & Lorenz, R. D. The temperature of Europa's subsurface water ocean. *Icarus* **168,** 498–502 (2004).
5. Goodman, J. C., Collins, G. C., Marshall, J. & Pierrehumbert, R. T. Hydrothermal plume dynamics on Europa: Implications for chaos formation. *J. Geophys. Res.* **109,** E03008 (2004).
6. Vance, S. & Brown, J. M. Layering and double-diffusion style convection in Europa's ocean. *Icarus* **177,** 506–514 (2005).
7. Vance, S. & Goodman, J. C. in *Europa* (eds Pappalardo, R. T., McKinnon, W. M. & Khurana, K. K.) 459–482 (Univ. Arizona Press, 2009).
8. Goodman, J. C. & Lenferink, E. Numerical simulations of marine hydrothermal plumes for Europa and other icy worlds. *Icarus* **221,** 970–983 (2012).
9. Kivelson, M. G. *et al.* Galileo magnetometer measurements: A stronger case for a subsurface ocean at Europa. *Science* **289,** 1340–1343 (2000).
10. Collins, G. & Nimmo, F. in *Europa* (eds Pappalardo, R. T., McKinnon, W. M. & Khurana, K. K.) 259–281 (Univ. Arizona Press, 2009).
11. Greenberg, R., Hoppa, G. V., Tufts, B. R., Geissler, P. & Riley, J. Chaos on Europa. *Icarus* **141,** 263–286 (1999).
12. McKinnon, W. B. Convective instability in Europa's floating ice shell. *Geophys. Res. Lett.* **26,** 951–954 (1999).
13. Pappalardo, R. T. & Barr, A. C. The origin of domes on Europa: The role of thermally induced compositional diapirism. *Geophys. Res. Lett.* **31,** L01701 (2004).
14. Schmidt, B. E., Blankenship, D. D., Patterson, G. W. & Schenk, P. M. Active formation of chaos terrain over shallow subsurface water on Europa. *Nature* **479,** 502–505 (2011).
15. Hussmann, H., Spohn, T. & Wieczerkowski, K. Thermal equilibrium states of Europa's ice shell: Implications for internal ocean thickness and surface heat flow. *Icarus* **156,** 143–151 (2002).
16. Beuthe, M. Spatial patterns of tidal heating. *Icarus* **223,** 308–329 (2013).
17. Heimpel, M. H. & Aurnou, J. M. Turbulent convection in rapidly rotating spherical shells: A model for equatorial and high latitude jets on Jupiter and Saturn. *Icarus* **187,** 540–557 (2007).
18. Aurnou, J. M., Heimpel, M. H., Allen, L., King, E. M. & Wicht, J. Convective heat transfer and the pattern of thermal emission on the gas giants. *Geophys. J. Int.* **173,** 793–801 (2008).
19. Julien, K., Knobloch, E., Rubio, A. M. & Vasil, G. M. Heat transport in low-Rossby-number Rayleigh–Bénard convection. *Phys. Rev. Lett.* **109,** 254503 (2012).
20. King, E. M., Stellmach, S. & Aurnou, J. M. Heat transfer by rapidly rotating Rayleigh–Bénard convection. *J. Fluid Mech.* **691,** 568–582 (2012).
21. Aurnou, J. M., Heimpel, M. H. & Wicht, J. The effects of vigorous mixing in a convective model of zonal flow on the Ice Giants. *Icarus* **190,** 110–126 (2007).
22. Soderlund, K. M., Heimpel, M. H., King, E. M. & Aurnou, J. M. Turbulent models of ice giant internal dynamics: Dynamos, heat transfer, and zonal flows. *Icarus* **224,** 97–113 (2013).
23. Lewis, E. L. & Perkin, R. G. Ice pumps and their rates. *J. Geophys. Res.* **91,** 11756–11762 (1986).
24. Moore, J. C., Reid, A. P. & Kipfstuhl, J. Microphysical and electrical properties of marine ice and its relationship to meteoric and sea ice. *J. Geophys. Res.* **99,** 5171–5180 (1994).
25. Oerter, H. *et al.* Evidence for basal marine ice in the Filchner–Ronne ice shelf. *Nature* **358,** 399–401 (1992).
26. Ojakangas, G. W. & Stevenson, D. J. Polar wander of an ice shell on Europa. *Icarus* **81,** 242–270 (1989).
27. Tyler, R. H. Magnetic remote sensing of Europa's ocean tides. *Icarus* **211,** 906–908 (2011).
28. Christensen, U. R. & Wicht, J. in *Treatise on Geophysics, Core Dynamics* Vol. 8 (ed. Schubert, G.) 245–282 (Elsevier, 2007).
29. Vance, S. & Brown, J. M. Thermodynamic properties of aqueous $MgSO_4$ to 800 MPa at temperatures from −20 to 100 °C and concentrations to 2.5 mol kg^{-1} from sound speeds, with applications to icy world oceans. *Geochim. Cosmochim. Acta* **110,** 176–189 (2013).
30. Kuang, W. & Bloxham, J. An earth-like numerical dynamo model. *Nature* **389,** 371–374 (1997).

Acknowledgements

This work was supported by the Institute for Geophysics of the Jackson School of Geosciences at The University of Texas at Austin (UTIG). Computational resources were provided by the NASA High-End Computing (HEC) Program through the NASA Advanced Supercomputing (NAS) Division at Ames Research Center. We thank M. Heimpel for providing the jovian-like model data in Fig. 1, T. Doggett for providing the geologic map of Europa in Supplementary Fig. 1, and J. Aurnou for providing Supplementary Fig. 2. This is UTIG contribution 2637.

Author contributions

K.M.S. and B.E.S. conceived of this project and wrote the paper. K.M.S. did all calculations and carried out the simulation. J.W. provided the numerical model and contributed to the convective regime transition arguments. D.D.B. contributed to the terrestrial analogue arguments. All authors discussed the results and commented on the manuscript.

Additional information

Supplementary information is available in the online version of the paper. Reprints and permissions information is available online at www.nature.com/reprints. Correspondence and requests for materials should be addressed to K.M.S.

Competing financial interests

The authors declare no competing financial interests.